Geochemistry Geophysics Geosystems G3
AN ELECTRONIC JOURNAL OF THE EARTH SCIENCES
Published by AGU and the Geochemical Society

Article
Volume 7, Number 2
28 February 2006
Q02N01, doi:10.1029/2005GC001070
ISSN: 1525-2027

Deep-water mass source and dynamic associated with rapid climatic variations during the last glacial stage in the North Atlantic: A multiproxy investigation of the detrital fraction of deep-sea sediments

M. Ballini and C. Kissel
Laboratoire des Sciences du Climat et de l'Environnement, Unité Mixte CEA/CNRS, Avenue de la Terrasse, F-91198 Gif-sur-Yvette Cedex, France (marine.ballini@lsce.cnrs-gif.fr)

C. Colin
Laboratoire Interactions et Dynamique des Environnements de Surface, Université de Paris XI, F-91405 Orsay Cedex, France

T. Richter
Royal Netherlands Institute for Sea Research, P.O. Box 59, 1790 AB Den Burg, Netherlands

[1] In order to investigate North Atlantic Deep Water (NADW) dynamics and variability during the last glacial stage, a very high resolution multiproxy analysis of the detrital fraction of sediments deposited during Heinrich event 4 and Dansgaard-Oeschger cycles 8 and 7 has been conducted on three deep-sea cores. These cores are distributed along the path of the North Atlantic Deep Water from the Faeroe Shetland Channel to the Reykjanes ridge and the Irminger basin. The concentration in fine-grained magnetites, the Ti-content, and the smectite percentage within the clay minerals show similar and coeval fluctuations at each site and are comparable from one site to the other. This is the imprint of the detrital fraction originating from the northern basaltic provinces and transported to the studied sites. The average grain size in the fine fraction indicates a transport by deep-sea currents. Therefore the observed fluctuations illustrate changes in the vigor of the bottom currents associated with the NADW with weak currents during cold periods (Heinrich 4 and stadials) and reactivation of the bottom circulation during interstadials.

Components: 8990 words, 8 figures, 1 tables.

Keywords: glacial period; Dansgaard-Oeschger cycles; North Atlantic; bottom water circulation; magnetic properties; clay minerals.

Index Terms: 3305 Atmospheric Processes: Climate change and variability (1616, 1635, 3309, 4215, 4513); 4962 Paleoceanography: Thermohaline; 4901 Paleoceanography: Abrupt/rapid climate change (1605); 1512 Geomagnetism and Paleomagnetism: Environmental magnetism.

Received 13 July 2005; **Revised** 21 September 2005; **Accepted** 22 November 2005; **Published** 28 February 2006.

Ballini, M., C. Kissel, C. Colin, and T. Richter (2006), Deep-water mass source and dynamic associated with rapid climatic variations during the last glacial stage in the North Atlantic: A multiproxy investigation of the detrital fraction of deep-sea sediments, *Geochem. Geophys. Geosyst.*, *7*, Q02N01, doi:10.1029/2005GC001070.

Theme: Past Ocean Circulation
Theme Editor: Laurent Labeyrie
Guest Editors: Jean Lynch-Stieglitz, Catherine Kissel, and Olivier Marchal

1. Introduction

[2] Over the last decade, the understanding of the interactions between the atmosphere, the ocean and the cryosphere during rapid climatic variations has been one of the main concerns of paleoceanographers and paleoclimatologists. Many studies have focused geographically in the North Atlantic and temporally on the last glacial period in order to determine the rate of Atlantic Meridional Overturning during these rapid climatic changes. Studies including stable isotopes [*Vidal et al.*, 1997, 1998; *Labeyrie et al.*, 1999; *Curry et al.*, 1999; *Dokken and Jansen*, 1999; *Elliot et al.*, 2002], foraminiferal assemblages [*Rasmussen et al.*, 1996a, 1996b], sediment mineralogy [*Moros et al.*, 1997, 2002], magnetic properties [*Kissel et al.*, 1999a, 1999b], grain-size distributions [*Prins et al.*, 2002; *Snowball and Moros*, 2003] were conducted, in the subpolar North Atlantic leading to the conclusion that at these latitudes the deep water mass has undergone rapid variations associated with the rapid climatic changes. However, the precise relationship between past changes in the meridional overturning rate and North Atlantic climate has not been resolved yet. Possible reasons for this are that these proxies have their own domain of applicability and their own limitations. For example, among the proxies used to monitor North Atlantic deepwater (NADW) circulation, benthic carbon isotopes are not independent of nutrient cycling and changes in the preformed chemistry. Other proxies, more directly controlled by deep water flow speed and mixing are therefore needed.

[3] In this context, the magnetic properties of sediments, coupled with other sedimentological proxies can be used as tracers for changes in the strength of the oceanic deep circulation. The magnetic records from sediment drifts from the region of the Faeroe Islands [*Rasmussen et al.*, 1996b, 1998; *Kissel et al.*, 1999a, 1999b], the Reykjanes Ridge [*Moros et al.*, 1997], the Irminger Basin and down to the Bermuda Rise [*Kissel et al.*, 1999a; *Laj et al.*, 2000] match the short-term oscillations observed in the oxygen isotopic record from Greenland ice cores. On the basis of the large geographical distribution of the sites, *Kissel et al.* [1999a] interpreted these short-term oscillations in the magnetic concentration as illustrating variable efficiency of the bottom current to transport the magnetite-rich sediment downstream from the northern basaltic source. Except for the magnetic properties, changes in the detrital sediment fraction, controlled by changes in the bottom current activity have been poorly investigated in that period of time. Changes in grain sizes have been proposed as reliable tracers [*Prins et al.*, 2002; *Snowball and Moros*, 2003] from the analyses of cores located close to the Reykjanes ridge. So far, the various sites have not been always investigated with the same proxies and not always with the same time resolution. This approach may lead to consider each core as a case study because it makes intercomparison of data and of sites very difficult.

[4] The purpose of this article is to investigate North Atlantic Deep Water (NADW) dynamics and variability during the last glacial stage using a very high resolution multiproxy analysis of different sedimentary sequences. Detailed magnetic investigations are here complemented by analysis of the clay fraction (XRD) and the entire terrigenous component (bulk sediment chemical composition (XRF) and grain size distribution). We focus on the time interval covering the H4 and D-O 8 and 7, representative of these short-term oscillations and clearly documented in three cores distributed along the NADW path from the southern Norwegian Sea to the Irminger Basin. The large geographical distribution of the cores and the fact that the same parameters are measured in the same way in each of them allow to distinguish the regional pattern from the local influences.

[5] Our various terrigenous proxies yield internally consistent results for each location, as well as closely similar patterns of variability between the three core sites along the NADW flow path. These imply changes in the vigor of bottom currents, with weak currents during cold periods (Heinrich 4 and stadials) and reactivation of the bottom circulation during interstadials.

2. Core Location and Characteristics

[6] The studied cores have been taken during various cruises within the framework of the international IMAGES program on board the R/V *Marion Dufresne* along the different branches of the NADW as they are described at present (Figure 1). The precise location of the cores is given in Table 1. Core MD95-2009 has been taken during the 1995 IMAGES 101 cruise. It is located along a contour current, just north of the Faeroe Shetland channel, directly under the influence of the Iceland-Scotland Overflow Water (ISOW) when it passes from the Norwegian Sea to the North Atlantic. The magnetic properties of this core have already been investigated at relatively low resolution [*Kissel et al.*, 1999a, 1999b; *Laj et al.*, 2000] and the content of

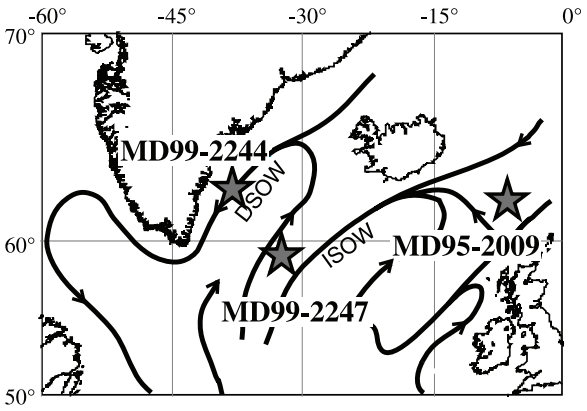

Figure 1. Schematic map of the North Atlantic Ocean showing the main path of the North Atlantic Deep Water and the location of the studied sites. DSOW, Denmark strait overflow water; ISOW, Iceland-Scotland Overflow Water.

ice-rafted material (IRD) has been reported by *Manthe* [1998]. Cores MD99-2247 and MD99-2244 have been taken during the 1999 IMAGES GINNA cruise. In the North Atlantic, the ISOW flows southward to the Charlie-Gibbs fracture zone where, following the topography, it goes back to the North along the western side of Reykjanes Ridge. Core MD99-2247 is located along this branch of the NADW in an area made of a succession of small sedimentary basins within the basaltic area of the medio-Atlantic tholeiitic ridge.

[7] Core MD99-2244 is from the Irminger Basin, along the Greenland slope. At this site, the sediment is bathed by the overflow water injected to the North Atlantic via the Denmark Strait (Denmark Strait Overflow Water, DSOW), and the NEADW forming a counterclockwise gyre along the Reykjanes ridge and the Greenland margin (Figure 1). It is very close to core SU90-24 studied using magnetic properties [*Kissel et al.*, 1999a, 1999b; *Laj et al.*, 2000] and stable isotopes and IRDs [*Elliot et al.*, 1998, 2001, 2002].

3. Sampling and Laboratory Methods

[8] The three cores have been sampled continuously with u-channels [*Tauxe et al.*, 1983; *Weeks et al.*, 1993]. Subsequent subsampling with small size discrete samples has been conducted more specifically in the interval on which we focus here in order to reach a higher resolution and to conduct multiproxy analyses on the same samples. These discrete subsamples were 1 cm slices taken closely from each other.

[9] The magnetic properties were first analyzed at a resolution of 4–5 cm using u-channels and 2G 255R cryogenic magnetometers within the shielded room of LSCE. The investigated magnetic parameters include the different remanent magnetizations (natural: NRM; anhysteretic: ARM; isothermal: IRM) and their stepwise demagnetization. The volume low field susceptibility (κ_{lf}) has also been measured with the same resolution. The laboratory procedures are given by *Kissel et al.* [1999b]. All the results obtained using u-channels are reported for the first time here except for those of core MD95-2009 already reported by *Kissel et al.* [1999a, 1999b] and *Laj et al.* [2000].

[10] The discrete samples were used to measure the low field susceptibility on dry sediment c_{lf}, and hysteresis parameters using an alternating gradient force magnetometer. The hysteresis parameters are the saturation magnetization (Ms), the saturation remanent magnetization (Mrs), the coercive force (Hc) and the remanent coercive force (Hcr). The dry samples were weighted so that c_{lf}, Mrs, and Ms are normalized by the mass of dry sediment. The reproducibility of these parameters within the same horizon is better than 5%. Finally, at representative depths, thermomagnetic experiments were conducted in high field using a horizontal Curie balance. An Ar flow was used throughout the experiment to avoid oxidation processes upon heating.

[11] The significance and importance of the magnetic parameters in paleoceanographic studies has been extensively discussed elsewhere [e.g., *Stoner et al.*, 1996; *Evans and Heller*, 2003]. Briefly, various parameters and parameters ratios yield information on the mineralogy, grain size and concentration of the magnetic fraction. These can then be used to infer provenance and transport

Table 1. Locations of the Studied Cores

Core	Latitude, °N	Longitude, °W	Water Depth, m	Sedimentation Rate, cm/kyr
MD95-2009	62°44.25′	3°59.86′	1027	32
MD99-2247	59°04.61′	31°28.34′	1690	40
MD99-2244	62°41.99′	37°33.73′	2110	22

pathways of the terrigenous component in deep-sea sediments.

[12] Clay minerals were identified by standard X-Ray diffraction (XRD) at the IDES laboratory (University of Paris XI), on the carbonate free clay sized particles (<2 μm size fraction) following the procedure described by *Colin et al.* [1999]. The semiquantification of the different clay mineral abundances has been obtained on glycolated diffractograms using the ''MacDiff'' software (R. Petschick, MacDiff software v.4.2.5, 2001; available at http://servermac.geologie.uni-frankfurt.de/Staff/homepages/Petschick/RainerE.html), by peak area calculation of the main clay minerals groups: smectite (001) including illite/smectite mixed-layered minerals (smectite sensu lato), characterized by a broad peak over 15–17 Å after glycolation, illite (001) 10 Å, kaolinite (001) and chlorite (002) 7 Å. Relative proportions of kaolinite and chlorite were determined on the basis of the ratios of the 3.57/3.54 Å peak areas. Then, the values have been converted into percentages of the total clay fraction (estimated by summing all the calculated peak areas). The precision of the semiquantification is estimated to be ±5%.

[13] Grain-size distribution measurements of carbonate- and biogenic silica-free sediments were carried out on a COULTER® Laser Particle Size Analyzer LS130 in the same laboratory. Bulk sediments were first decarbonated via reaction with HCl, followed by successive washing with distilled water. Sediments were then reacted with 1 N Na_2CO_3 solution to remove biogenic silica. The reaction was performed in a water bath at a temperature of 85°C for 4 hours. The Na_2CO_3 solution was then neutralized by a series of distilled water rinsing steps followed by centrifugation.

[14] The changes in major and trace elements in the sediment has been obtained by profiling X-Ray fluorescence, using the Avaatech XRF core-scanner at the Royal Netherlands Institute for Sea Research (NIOZ) [*Richter et al.*, 2005]. The measurements were made on u-channels, every 0.5 cm for core MD99-2244 and 1 cm for core MD99-2247. The XRF data of core MD95-2009 were obtained using the CORTEX core scanner, which is a machine of the preceding generation [*Jansen et al.*, 1998].

[15] The ice rafted debris (IRD) have been counted in core MD99-2247 and are expressed in number of lithic grains coarser than 150 μm per gram of dry sediment. We have transferred on core MD99-2244 the same parameter obtained from the twin core SU90-24 [*Elliot et al.*, 1998, 2001] using the correlation of the magnetic susceptibility records.

4. Stratigraphy of the Studied Interval

[16] High resolution precise stratigraphy in this time interval is a difficult task because the known climatic features, in particular surface ocean parameters, are not always synchronized [*Elliot et al.*, 2001]. Radiocarbon ages can also be biased by temporal and spatial variability of ^{14}C reservoir ages. Therefore, in order to define in each core the different rapid climatic events (H4 and D-O cycles 8 and 7) on which we focus our high resolution multiproxy study, we use the magnetic records as a guide (Figure 2).

[17] The rationale for this is that at mid-high latitudes, and along the path of the NADW, it has been shown that not only the Heinrich events but also the more rapid climatic events are recorded in the concentration-dependent magnetic parameters [*Rasmussen et al.*, 1996b, 1998; *Moros et al.*, 1997; *Kissel et al.*, 1999a, 1999b]. These fluctuations have been tied to the Greenland GISP2 ice record [*Kissel et al.*, 1999a] showing that, at these sites, the cold events over Greenland corresponding to the Heinrich events [*Bond et al.*, 1993] and the cold phase of each Dansgaard/Oeschger event (stadial) coincide with intervals of low magnetic concentration [*Kissel et al.*, 1999a, 1999b].

[18] In addition to this general association between cold events and low magnetic concentration in sediments from mid-high latitudes [*Kissel et al.*, 1999b], it has also been shown that the interval on which we focus here is well bracketed by changes of the earth magnetic field [*Laj et al.*, 2000]. In particular, two clear geomagnetic features are present during marine isotopic stage 3, the Mono-Lake event (or low intensity event p5 [*Kent et al.*, 2002]) and the Laschamp event [*Laj et al.*, 2000]. In both ice cores and marine sediments, the low intensity event p5 is recorded between interstadials 7 and 6 and the Laschamp event at the end of interstadial 10 [*Laj et al.*, 2000; *Wagner et al.*, 2000]. The Heinrich event 4 and the D-O cycles 8 and 7 are thus occurring between these two climatically independent tie points used to ascribe a chronostratigraphic scale to the magnetic records used here.

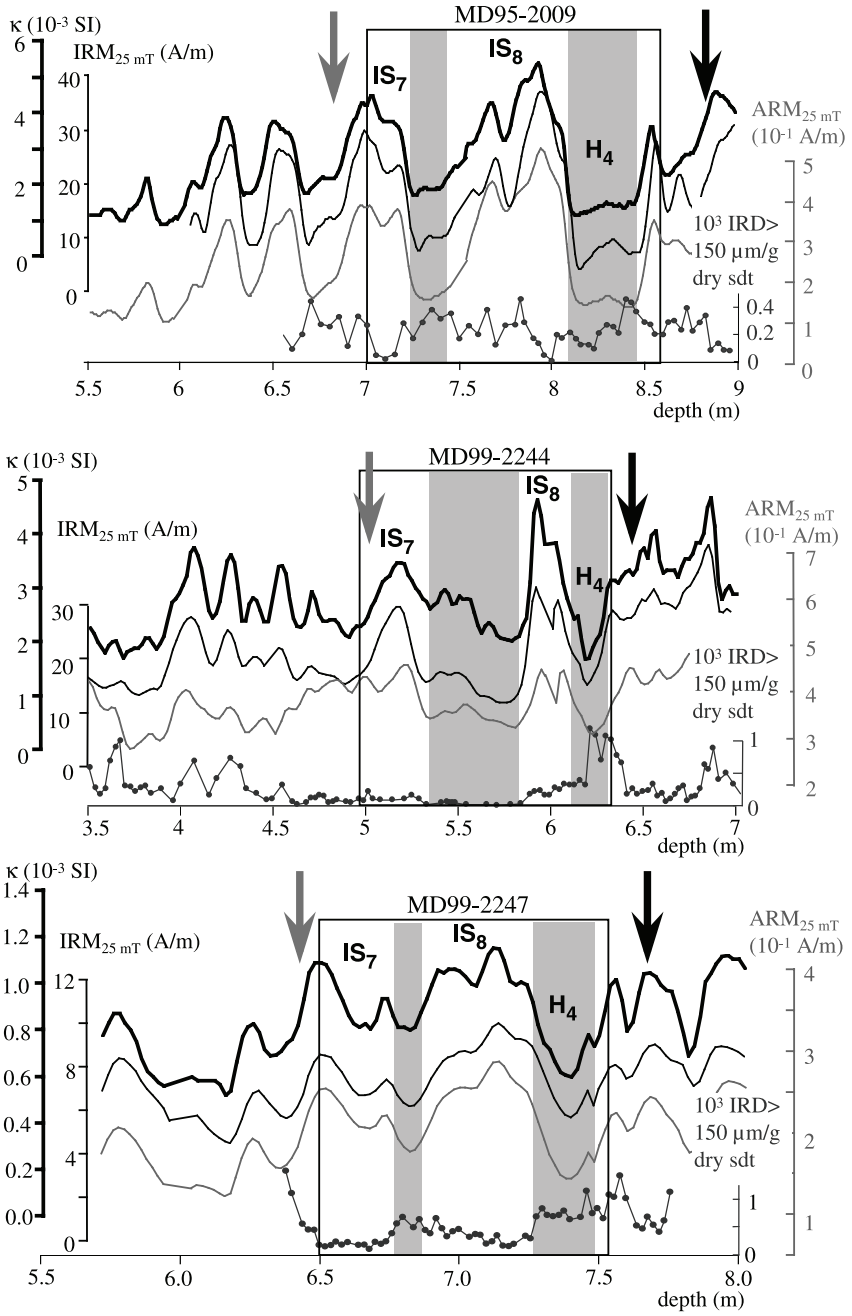

Figure 2. Long-term trends on the magnetic parameters κ, IRM, and ARM measured on u-channels (see text). For each core the IRD content is also reported at the bottom of each diagram. They have all been determined by counting the fraction >150 µm and normalizing it by the dry mass of the sediment. The IRD data reported for core MD99-2244 have been obtained from core SU90-24 (see text). The studied depth interval is indicated by the rectangle which is located between the Laschamp event (black arrow) and the Mono Lake feature (gray arrow). The gray areas are showing the cold intervals (stadials and Heinrich events).

[19] In the three studied cores, the Laschamp event is very well marked by a large swing in inclination and a drop in the normalized intensity record. The Mono-Lake intensity low is also clear except in core MD99-2244 from the Irminger basin where a low is observed but less pronounced than in the other cores. The depth at which the Laschamp event and the Mono Lake intensity low are observed in the cores are shown by the vertical thick arrows in Figure 2 where the bulk magnetic records, measured on u-channels, are also reported.

[20] We identify the Heinrich event 4 as the major minima in the magnetic records following the Laschamp event. It is most of the time also characterized by a high IRD content although the latter may start before the occurrence of the magnetic minima as already noticed by *Elliot et al.* [2001]. The two Dansgaard-Oeschger cycles following the Heinrich event 4 (D-O 8 and 7) are defined as the two main maxima/minima magnetic cycles between Heinrich event 4 and the Mono Lake intensity low (gray arrow). Depending of the cores, the stadials of the Dansgaard-Oeschger cycles are or are not characterized by IRD events. When the minimum seemed to be double as for stadial 7 in core MD99-2247, we defined it consistently with the peaks in the IRD content.

[21] The depth intervals on which our high resolution multiproxy analysis is focused on is indicated in Figure 2 by the rectangles and it extends over 1.6 m, 2 m and 1.3 m in cores MD95-2009, MD99-2247 and MD99-2244, respectively. The average sedimentation rates calculated using the ages given for these intervals in the Greenland ice records are reported in Table 1. Our centimetric high resolution sampling reaches a resolution of a maximum of 45 years.

5. Results

5.1. Nature of the Magnetic Minerals

[22] In each core, we imparted a backfield of −0.3T on previously saturated samples (with 1T field). The ratio between these two IRM values (S-ratio = $(-IRM_{0.3T})/IRM_{1T}$)) provides a measure of the relative amount of magnetically ''hard'' minerals (high-coercivities) to ''soft'' minerals. The S-ratio we obtained are invariably close to 1 (Figure 3), indicating that low coercivity (magnetically ''soft'') minerals are dominant with no major changes with time. Thermomagnetic curves obtained from representative samples from the Heinrich interval, from the interstadials and from the stadials (Figure 4) show that these low coercivity minerals lose their magnetization around 580°C–600°C. This is typical for magnetite. The reversibility of the curves is variable with most often a cooling curve less magnetized than the heating one. This only indicates that despite the use of Ar, oxidation could not be entirely avoided upon heating. In some cases, on the contrary, the cooling curve is slightly higher than the heating one (stadial and interstadial in core MD99-2244 and interstadial and Heinrich in core MD99-2247). In these cases, although no inflexion point is observed during heating, the more magnetized cooling curve may illustrate some exsolution process of Ti-rich magnetites upon heating. This would indicate that larger amounts of Ti-rich magnetites are deposited at these sites compared to the other sites.

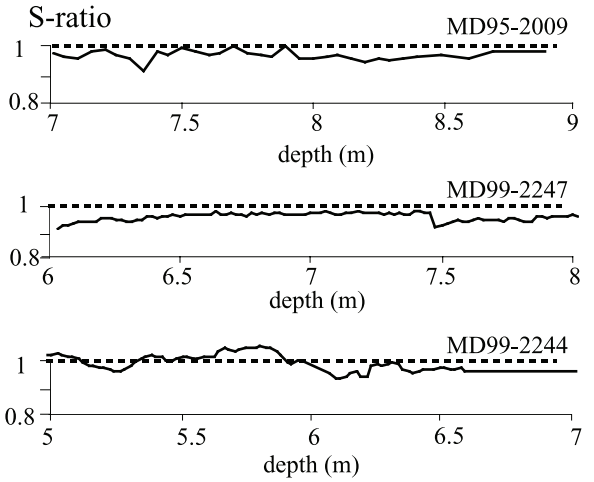

Figure 3. S-ratio obtained in the different cores showing the uniformity of the magnetic minerals all over the studied interval.

[23] At each site, the different curves are very similar, confirming that no major change in the nature of the magnetic minerals occurred with time during the rapid climatic events.

5.2. Magnetic Grain Size

[24] When magnetite is the dominant magnetic mineral, its domain state can be determined using magnetic hysteresis parameters. The domain state of magnetites is related to the size of the grains with increasing grain size from single domain (SD) to pseudosingle domain (PSD) to multidomain (MD). For all the studied cores, when the magnetization ratio (Mrs/Ms) is reported versus the coercivity ratio (Hcr/Hc) [*Day et al.*, 1977] (Figure 5), the data plot within the pseudosingle domain (PSD) field, which characterizes grains of a few micrometers as an average.

[25] In core MD99-2247, the Mrs/Ms ratio is on average larger than in the other cores and this is associated with lower Hcr/Hc ratios. This indicates that while the magnetites have similar average grain sizes in cores MD95-2009 and MD99-2244,

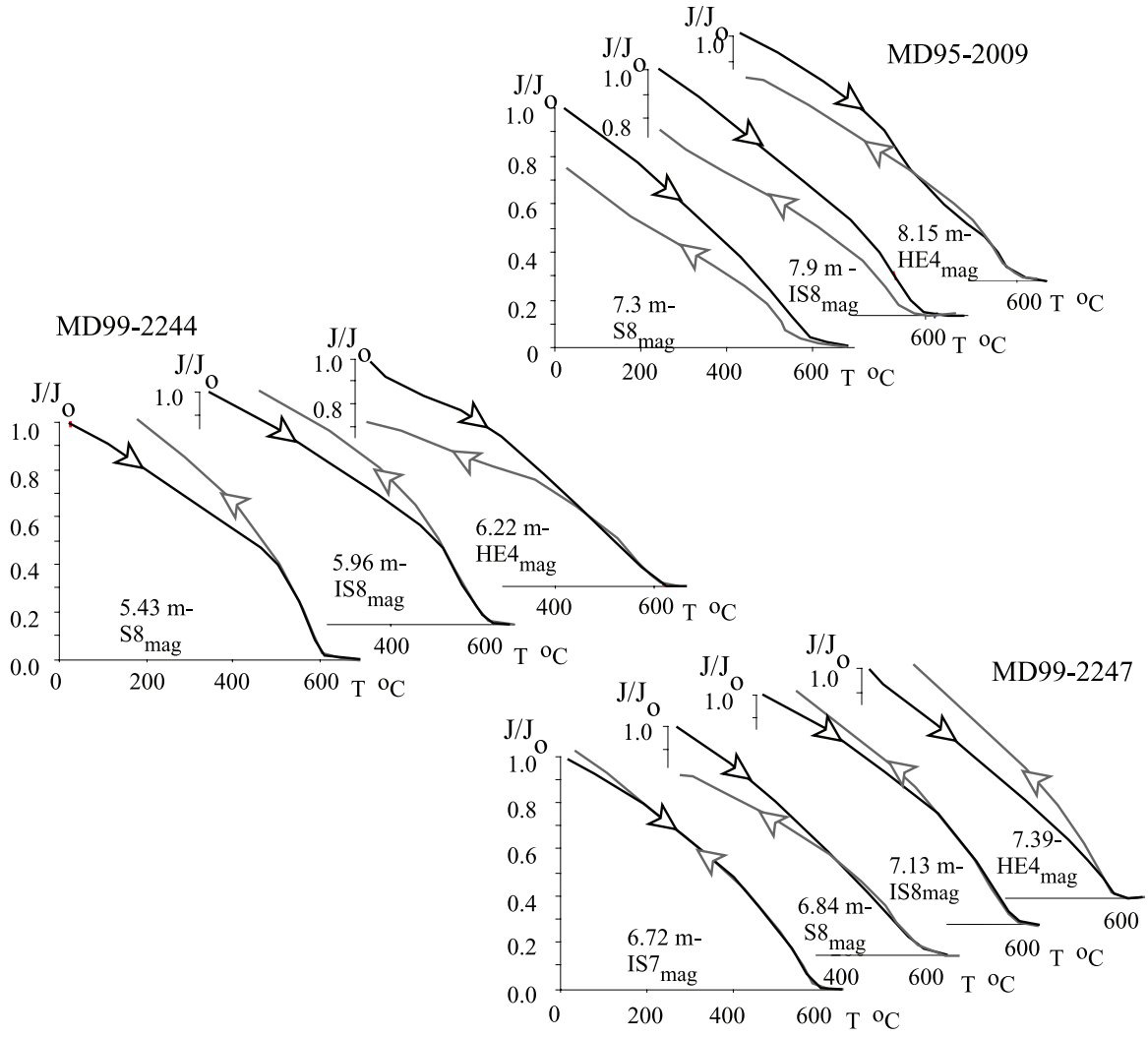

Figure 4. Thermomagnetic curves obtained for each core at different depths also corresponding to different phases of the rapid climatic changes. The induced magnetizations are normalized to the initial one. Black (gray) curves are for the heating (cooling) part of the cycles.

they are smaller in core MD99-2247 from the Reykjanes Ridge.

[26] A very small scatter of the points is observed in each diagram. Although this scatter does not correspond to a distribution along a single hyperbole, we may in a first approximation attribute it to subtle changes in the average magnetic grain size. In order to get a closer view of these subtle changes and of their distribution with depth at each site, we reported in Figure 6 the Mrs/Ms with a reversed scale together with the low field susceptibility record (χ_{lf}) measured on discrete samples as a visual guide for the changes in magnetic concentration. The changes in the Mrs/Ms ratio have about the same amplitude as those reported by *Snowball and Moros* [2003] for the Reykjanes ridge. However, the pattern we observe is different from the one of Snowball and Moros and different from one core to another. HE4 is not associated with the finest grains all over the interval but it is characterized either by a decrease (MD99-2247 and MD95-2009) or by an increase (MD99-2244) in the grain size of magnetites. So the finest magnetic grains are observed at the beginning or during HE4 (core MD99-2244) or at the HE4/IS8 transition (MD99-2247) or at the onset of IS8 when the magnetic susceptibility is at a maximum (core MD95-2009). It then progressively increases until the end of the stadial S8 (core MD99-2244) or the end of the interstadial IS8 marking in that case a plateau with relatively coarser grains during S8 (MD95-2009 and MD99-2247). In all cases,

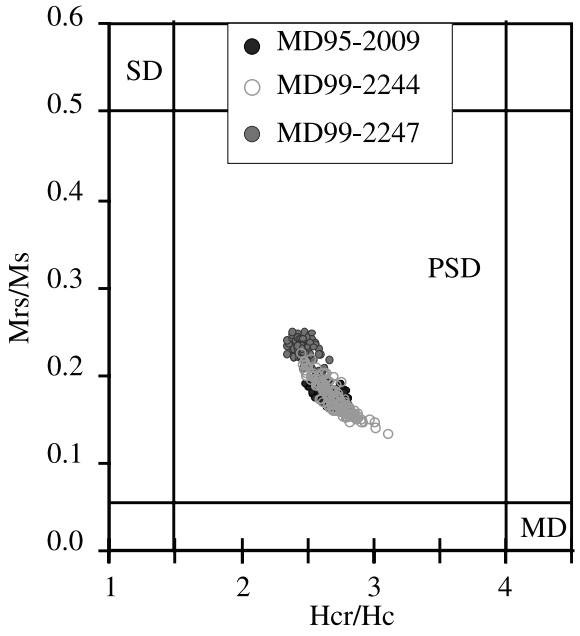

Figure 5. Hysteresis parameters reported in the diagram proposed by *Day et al.* [1977]. SD, PSD, and MD are for single domain, pseudosingle domain, and multidomain.

this is followed by a sharp decrease in the magnetic grain size at the transition with the IS7.

5.3. Magnetic Concentration

[27] As shown above, the changes observed in the magnetic grain sizes are far too small to have a significant impact on the changes in the magnetic parameters like ARM, IRM (or Mrs), Ms, κ_{lf} and χ_{lf}. Therefore, in these cores, all these parameters are essentially controlled by changes in magnetic concentration. This is confirmed by the very identical patterns of ARM, IRM and κ data obtained from u-channels with a resolution of 4–5 cm (Figure 2) and of c_{lf} and Mrs data obtained at high resolution (Figure 6).

[28] Cores MD99-2244 and MD95-2009 are the most magnetized with c_{lf} varying from 2.4 to 5.9 $\mu m^3.kg^{-1}$ and 1.3 to 5.7 $\mu m^3.kg^{-1}$, respectively, compared to 0.77 to 2.1 $\mu m^3.kg^{-1}$ in core MD99-2247. The highest values of each core are in the range of values obtained in these area for present-day sediment (1 to 6 $\mu m^3.kg^{-1}$ [*Watkins and Maher*, 2003]).

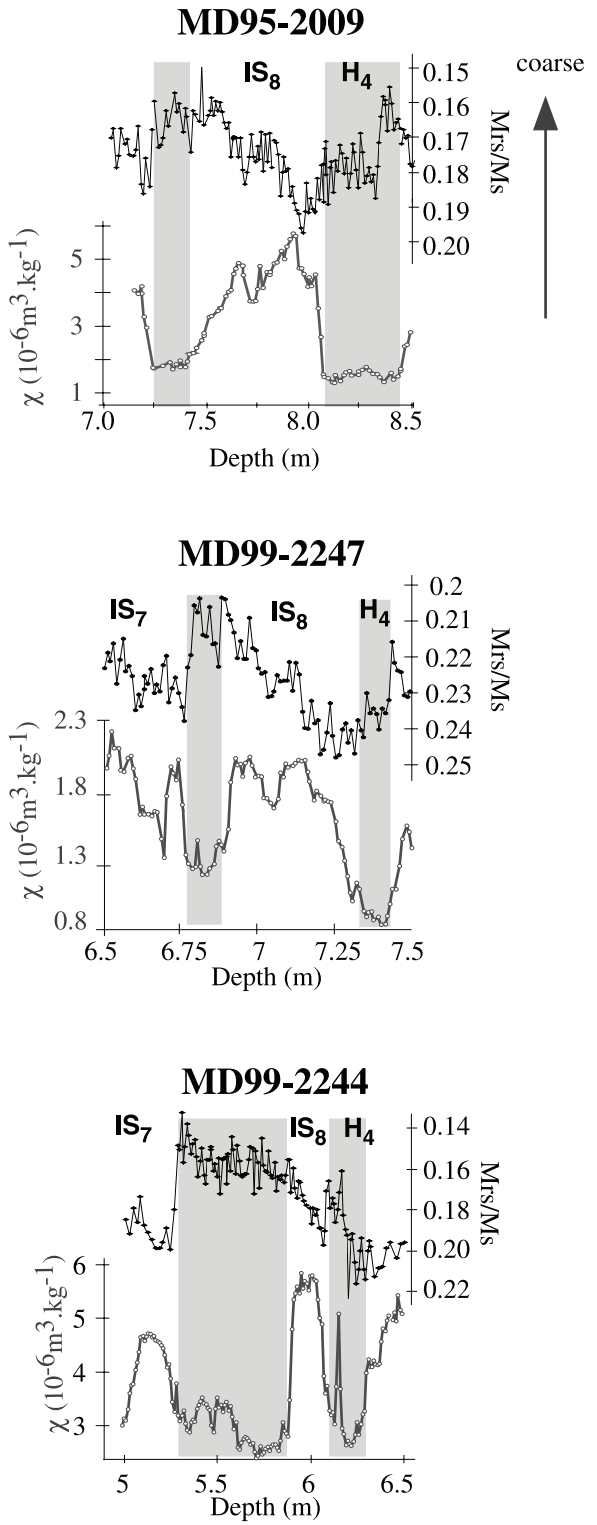

Figure 6. Comparison between the low field magnetic susceptibility measured on discrete samples and the grain size proxy Mrs/Ms. The gray areas show the cold intervals (Heinrich event 4 and stadials).

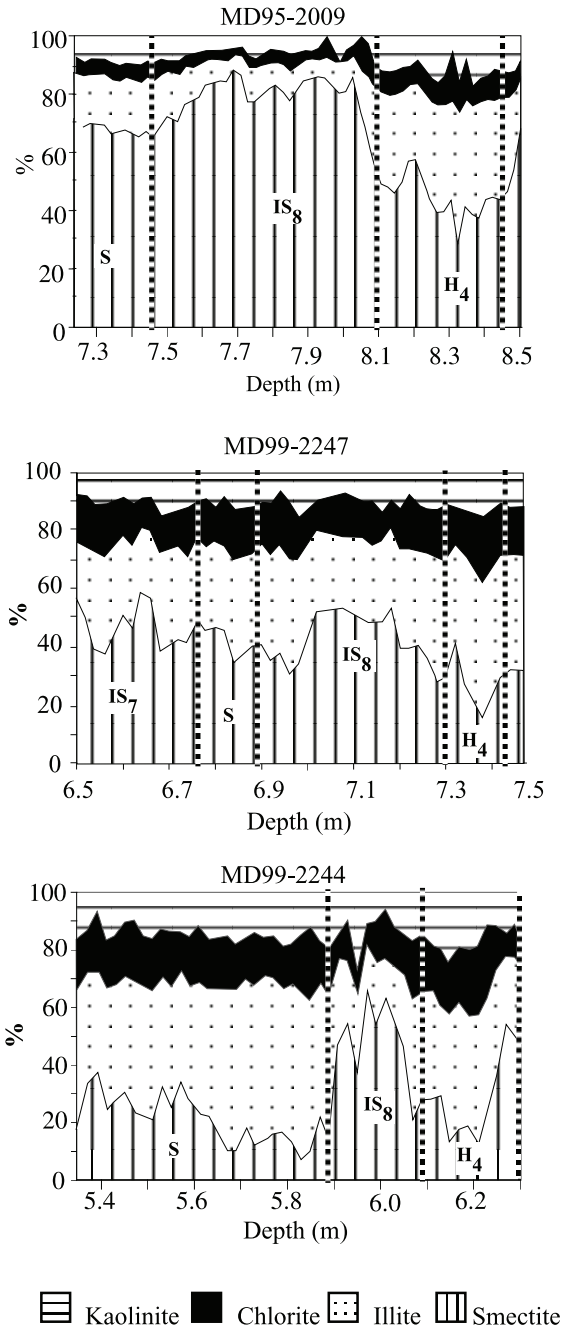

Figure 7. Clay content in each core. The dashed vertical lines are separating the different warm/cold periods from each other.

[29] Although the parameters have different absolute values from one core to another and identical patterns within each core, some differences in the shape of each event are sometimes observed at the different sites. If HE4 has the same signature in all the cores, IS8 can be described either by a broad maximum, as in core MD99-2244, or by a double structure as in cores MD95-2009 and MD99-2247. As in the preceding cycle, IS7 is defined either by a single peak (core MD99-2244), or by a double structure.

[30] These small differences observed in the details of the shape of the events are probably influenced by different local sedimentation rates. Despite these small discrepancies in the shape of the minima/maxima, it appears that the broad magnetic pattern is similar in these cores recovered from different geographical areas. The regional significance of these fluctuations, already discussed at low resolution by *Kissel et al.* [1999a] is confirmed here.

5.4. Clay Mineralogy and Major Elements

[31] The clay mineral assemblages in every studied core consist mainly of illite, chlorite, kaolinite and smectite (s.l.). We can also observe local presence of trace amounts of mixed-layered illite/vermiculite in core MD99-2244 from the Irminger basin.

[32] The relative abundance of the main minerals, illite, smectite, kaolinite and chlorite is reported in Figure 7. In core MD95-2009, smectite (30–90%) is the dominant clay mineral, with high amplitude fluctuations. Illite represents 5 to 45% of the clay size fraction, and kaolinite and chlorite are in minor abundance (0 to 13% and 0 to 17%, respectively). In general, illite, chlorite and kaolinite concentrations are similar and inversely correlated to the smectite abundance distributions. In this core, the clay mineral distribution indicates a narrow correlation with the magnetic parameters. IS8 is characterized by higher contents of smectite (60–85%) than HE4 (30–60%) and S8 (65–70%).

[33] The same pattern, but even more pronounced is observed in core MD99-2244 with smectite varying between 67% during IS8 (against 14% for illite) and 7% during HE4 and during S8 (against 58% for illite). In this core, chlorite and kaolinite only represent 8–27% and 5–14%, respectively.

[34] In core MD99-2247, the smectite content varies from 15 to 60%, inversely correlated to illite ranging between 20 to 47%, chlorite (8 to 22%) and kaolinite (7 to 15%). In this core, the HE4 is also characterized by a low concentration of smectite with respect to illite. This proportion is inverted during IS8 and these relative fluctuations are superimposed to a continuous increase in the smectite percentage.

[35] Though kaolinite and chlorite contents present a general trend similar to that of illite, their low content and amplitudes allow us to use only the smectite/illite ratio to represent the mineralogical changes within the clay fraction. In the three cores, the smectite/illite ratio variations are similar to those of the magnetic parameters. In general, IS8 are characterized by higher smectite/illite ratio than HE4 and S8.

[36] The Xrf scanning gave us access to semiquantitative estimations of the titanium and potassium content. In core MD99-2244 the Ti content is higher than in core MD99-2247. Core MD95-2009 has been measured with a different apparatus, and therefore the quantitative comparison is not possible. In all the cores, the Ti content is broadly anticorrelated to the K content. As described by *Richter et al.* [2005] for a core from the Faeroe Shetland channel, close to core MD95-2009, the Ti/K XRF intensity ratio illustrates the balance between basaltic (high Ti) and continentally derived ''acidic'' (high K) sources. Likewise, it shows in the three studied cores recurrent large amplitude short-term fluctuations illustrating a relatively stronger basaltic contribution to the bulk sediment during interstadials than during Heinrich event 4 and stadial intervals (Figure 8). This is strikingly similar to what is observed in the smectite content and the magnetics.

5.5. Grain Size Distribution

[37] Following *Snowball and Moros* [2003] and in order to compare with their data, we selected the mean of the size fraction 0.5–10 μm within the total fraction. As mentioned by the authors, the rationale for this is given by *Prins et al.* [2002], who demonstrated that in a region submitted to iceberg melting, the grain size distributions are described by mixtures of poorly sorted ice rafted detritus and current-sorted fine fraction among which the fraction with a peak distribution <10 μm. According to these authors, this fraction is therefore a better proxy of the behavior of low energy bottom-currents than the sortable silt [*McCave et al.*, 1995] in glacial subpolar North Atlantic. Smaller is the mean in this size fraction, weaker is the bottom current. The results are reported in Figure 8. In cores located at the two edges of the investigated area (MD95-2009 and MD99-2244), the similarity between the grain size <10 μm curve and the other curves is remarkable. In core MD99-2247, the record is consistent with the others during H4 and IS8 and it then exhibits high amplitude variations during the end of IS8, S8 and IS7.

6. Discussion

[38] All the data obtained at high resolution allow us to determine the provenance of the sedimentary assemblages and the possible mechanisms by which they were transported to the sites. Below, we will show that our results can be primarily interpreted in terms of fluctuations of bottom current vigor, and that other transport pathways of terrigenous material are at most of minor importance throughout the time period investigated in this study.

6.1. Sediment Provenance

[39] As shown in Figure 8, the main characteristic that is emphasized by this high resolution multiproxy investigation is the coeval variations in the concentration of magnetic minerals, clearly identified as pseudo-single domain magnetites, in the relative percentage of smectite within the clay mineral assemblages and in the Ti/K ratio. This is verified at each site, at very different geographical locations, along different branches of the North Atlantic Deep Water and therefore constitutes a regional sedimentological signature. Obviously, it indicates that magnetites, smectites and Ti-rich mineralogical fraction originate from a single common source.

[40] One of the main petrological province in the subpolar North Atlantic is the volcanic area constituted of Iceland, the Faeroe Islands and the eastern part of Greenland, all dominated by Tertiary and Quaternary basaltic rocks. The sediments resulting from the alteration of these basalts are very rich in magnetites [*Pouthiers and Gonthier*, 1978; *Kissel et al.*, 1999a; *Watkins and Maher*, 2003] and are characterized by high Ti content [*Lavrov et al.*, 1971; *Latouche and Parra*, 1976, 1979; *Grousset et al.*, 1982; *Lackschewitz et al.*, 1994]. Smectite is largely of detrital origin in the North Atlantic [*Behairy et al.*, 1975], where it is derived from different sources and processes [*Biscaye*, 1965; *Griffin et al.*, 1968; *Chamley*, 1989; *Fagel et al.*, 2001]. In the subpolar North Atlantic, highest smectite concentrations occur in the region of Iceland and Faeroe-Shetland islands [*Latouche and Parra*, 1976, 1979; *Grousset et al.*, 1982; *Parra*, 1980; *Parra et al.*, 1986]. Therefore the mineralogical assemblage composed of magnetites, smectites and Ti-rich fraction, as identified

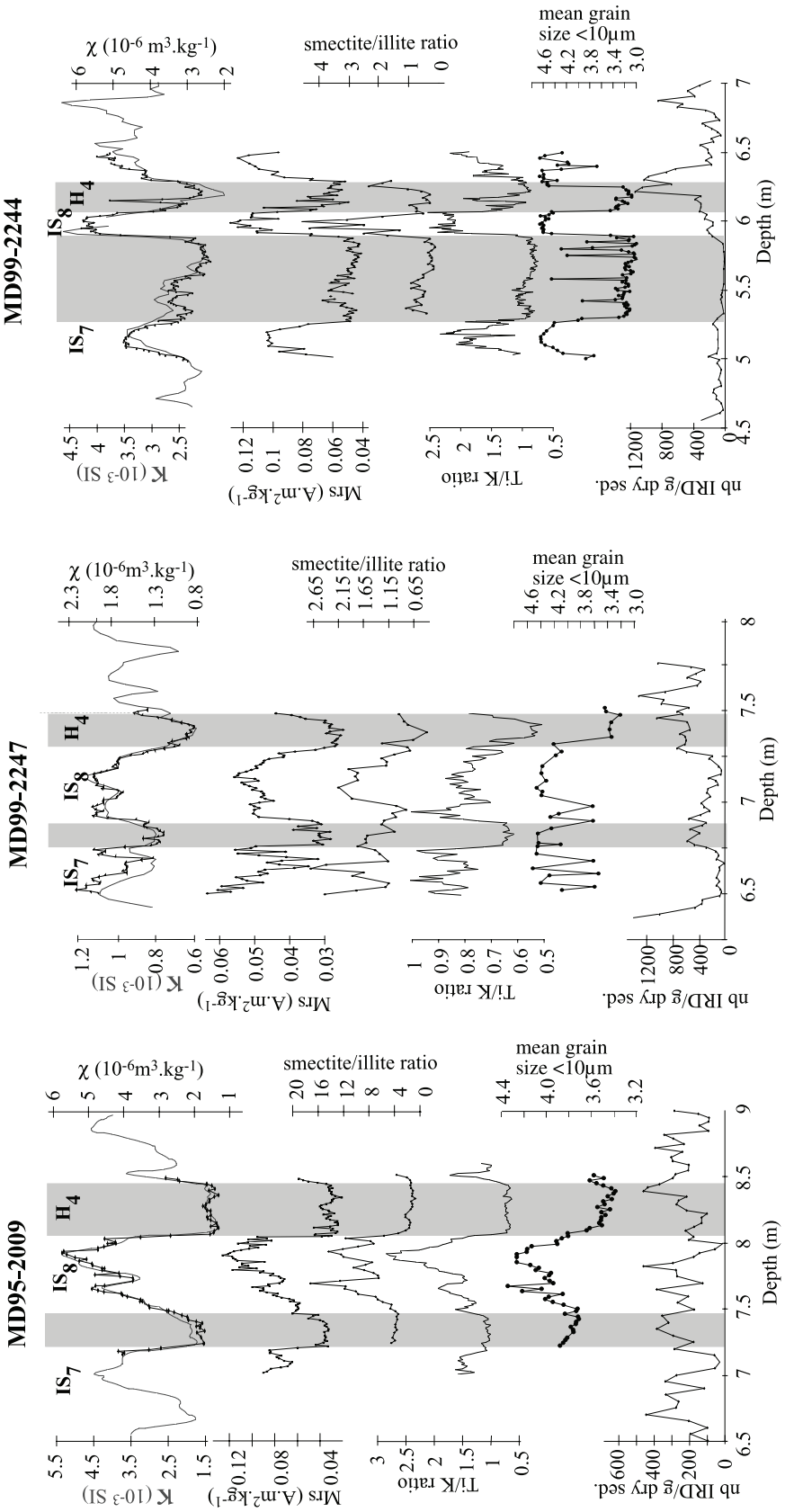

Figure 8. Synthesis of the data obtained from the three cores and which have a regional meaning in terms of variability of the bottom current strength (see text). For each core the IRD content is also reported in the bottom part. The cold periods H4 and S8 are highlighted by gray rectangles.

in the three studied cores, clearly corresponds to the fraction of the sediment originating from the weathering of these basaltic rocks.

[41] This assemblage alternates in the sedimentary sequence with a mineralogical fraction rich in potassium and characterized by illite and chlorite. In the subpolar North Atlantic, these clay minerals derive from the physical erosion or moderate chemical weathering of the Canadian and Scandinavian shields, Baffin Island, Scotland, Ireland and Greenland [*Biscaye*, 1965; *Griffin et al.*, 1968; *Rateev et al.*, 1969; *Petersen and Rasmussen*, 1980; *Chamley*, 1989]. Kaolinite, which represents a minor component of the clay fraction, is also essentially inherited from the adjacent landmasses where it formed during preglacial times [*Berry and Johns*, 1966; *Chamley*, 1989].

6.2. Transport by Bottom Currents

[42] Sites MD99-2244 and MD99–2247 are located south of the volcanic source area which implies that their basaltic–derived fraction is allochthonous and has been transported southward.

[43] Eolian transport cannot play an important role here as the emerged basaltic areas were covered by ice during the last glacial period and could not deliver at sea magnetite concentrations as high as the one observed in the cores. Moreover, the most significant inputs of eolian dusts in the North Atlantic are observed at much lower latitudes [*Moreno et al.*, 2002; *Watkins and Maher*, 2003]. The remaining possible transport vectors of the basaltic fraction are either the near-bottom currents associated with the different branches of the North Atlantic Deep Water [*Fagel et al.*, 1996; *Fagel and Hillaire-Marcel*, 1997; *Gehrke et al.*, 1996; *Revel et al.*, 1996; *Moros et al.*, 1997; *Rasmussen et al.*, 1998; *Kissel et al.*, 1999a] or the vertical advection by iceberg melting [*Robinson et al.*, 1995; *Stoner et al.*, 1996; *Watkins and Maher*, 2003].

[44] Magnetic IRDs are identified, both in surface [*Watkins and Maher*, 2003] and in glacial sediments [*Kissel*, 2005, and references therein] as coarse-grained magnetites of multidomain type. These grains have never been found in the area and water depths concerned by the overflow water mass which, on the contrary is characterized by very subtle changes in magnetic grain size within the pseudo-single domain range [*Kissel et al.*, 1999a, 1999b; *Snowball and Moros*, 2003; *Watkins and Maher*, 2003]. In addition, in the cores studied here, the horizons characterized by high IRD content are those in which the basaltic component is weak. Therefore the main ice rafting events which coincide with the illite and chlorite delivery, are not originating from the basaltic areas but rather from the surrounding continents.

[45] Consequently, for the basaltic detrital fraction, we better invoke a resuspension of previously well sorted material within the basaltic provinces and its subsequent transport by near-bottom currents. The remarkable agreement between the bottom flow speed indicator (mean grain size <10 μm) and the basaltic component indeed shows that this transport vector is the best candidate. This is also consistent with the observation made by *Watkins and Maher* [2003] on core tops that the magnetic fraction in modern sediments along Reykjanes Ridge (their cluster 1) is derived from "bottom water transport by ISOW". Although we deal here with a completely different time period which also means a different climatic context, the two observations converge.

[46] A final argument for the transport by deep currents from a single source downstream is illustrated by the decrease in the concentration of magnetites and in their average grain size from core MD95-2009 to core MD99-2247. This illustrates a progressive deposition along the NADW flow path of first abundant and relatively coarse magnetic grains close to the source and of less and finer grains further downstream. At the western side, a new detrital input transported by the Denmark Strait Overflow Water is observed with higher concentrations and slightly coarser magnetic particles in the Irminger Basin (core MD99-2244) compared to the Reykjanes Ridge.

6.3. Time Evolution and Dynamic of the Bottom Current

[47] The temporal changes in the concentration of the basaltic fraction can result either from changes in the strength of the bottom current as already suggested at longer timescale [*Moros et al.*, 1997, 2002; *Rasmussen et al.*, 1998; *Kissel et al.*, 1999a, 1999b] or from dilution by biogenic or by other nonmagnetic components. Dilution by biogenic fraction is very unlikely as the number of diatoms decreases during Heinrich event 4 when the basaltic fraction is also weak (S. Nave et al., Primary productivity response to abrupt climatic changes (Heinrich events) at the northern North Atlantic, submitted to *Paleoceanography*, 2005) and the changes in the calcium carbonate content are far too small (a few%) at these latitudes [*Rasmussen et*

al., 1998] to account for such changes in the basaltic concentration. Nonbasaltic ice rafting detrital delivery may have lowered the concentration of the basaltic component during cold events (Heinrich and stadials). However, such ice rafting events are not always occurring or not always synchroneous with intervals of low basaltic content [*Elliot et al.*, 2001]. Therefore, while the continental derived material certainly modulates the basaltic signature in the studied sediment cores, it cannot account entirely for the observed pattern from east to west North Atlantic. In other words, it seems unrealistic to envisage a perfectly constant and continuous basaltic-derived sedimentation all along the NADW flow path, periodically diluted by ice-rafted input of continentally derived nonbasaltic material. Consequently, our interpretation is that the observed temporal fluctuations in the concentration of the basaltic fraction at each site result from regional-scale changes in the strength of the deep-sea current. This interpretation is strongly supported by the grain size analyses (<10 μm), as the mean of this size fraction systematically decreases (increases) during intervals with reduced (enhanced) input of basaltic material. *Snowball and Moros* [2003] also suggested that, because of the possible dilution effect on the concentration-dependent parameters, the magnetic grain size would be a better proxy of changes in bottom current strength in the same way as the mean grain size <10 μm, i.e., coarse (fine) grains would illustrate enhanced (reduced) bottom current strength. At the sites they studied close to Reykjanes Ridge, the second order trend in the magnetic grain size is similar to that of the mean grain size and the magnetic concentration. In addition, the authors observe a saw tooth profile with larger grains at the end of the interstadials which would illustrate a progressive enhancement of the bottom current. Our high resolution magnetic grain size data are different (Figure 6). Following the interpretation of *Snowball and Moros* [2003], they would indicate, at our sites, a reduced bottom current at the beginning of H4 (MD99-2244) or at the inception of IS8 (MD99-2247) or during IS8 (MD95-2009). At all of our sites, relatively coarse magnetic grains are observed during S8, which would imply enhanced bottom currents, in complete contradiction with all the other proxies. We have no explanation why our results differ from the ones of *Snowball and Moros* [2003], except that we measured at very high resolution so that each event is documented by a large number of points allowing a more precise comparison with the other proxies. The differences observed in the magnetic grain size patterns, in addition to the fact that they only correspond to very small variations, indicate that this parameter does not have a consistent regional meaning and cannot be used to decipher deep current dynamics at a regional scale. The distribution of the basaltic-derived terrigeneous fraction and of the mean grain size <10 μm remain reliable proxies.

[48] The time evolution of these distributions during rapid climatic changes shows that the ability of the bottom-current to transport basaltic sediments along the path of the North Atlantic Deep Water, in other words, the strength of this current has significantly changed with time through successive Heinrich and Dansgaard-Oeschger events. It was reduced during the cold events compared to interstadials. Although benthic $\delta^{13}C$ records are scarce in the subpolar North Atlantic during this time period, they consistently show a reduced ventilation at least during H4 [*Elliot et al.*, 2002]. The same conclusion was reached at lower latitudes for H4 [*Vidal et al.*, 1998] and for both Heinrich events and stadials [*Keigwin and Boyle*, 1999].

[49] Although the ice cover was large during glacial time, the results obtained from core MD95-2009 indicate that the Norwegian Sea participated to this scenario with an active overflow from the Norwegian Sea toward the North Atlantic during interstadials. This is consistent with the suggestion of an open convection in this area during the warm part of the Dansgaard-Oeschger cycles based on faunal, isotopic and sedimentological data [*Rasmussen et al.*, 1996a, 1996b, 1998; *Dokken and Jansen*, 1999]. Our data supports the hypothesis that several circulation modes existed during the Dansgaard-Oeschger cycles, associated with shifts of the convection sites. The thermohaline circulation dynamic would therefore oscillate between a "glacial" mode, in which the convection sites would be located south of the Greenland-Iceland-Scotland sill, and a "warm" mode with open-ocean convection in the Nordic seas [*Alley and Clark*, 1999; *Sarnthein et al.*, 2000; *Ganopolski and Rahmstorf*, 2001]. The models suggest a total collapse of the NADW production during Heinrich events. If our data shows a strong reduction of the deep water dynamic, at least during these periods, the basaltic content is not null. It is in any case higher than in the intervals characterizing the Heinrich events in the Ruddiman belt only fed by iceberg melting. Therefore our interpretation is that

these low values cannot only result from iceberg discharges and that some basaltic material is still conveyed to the sites. This suggests that a weak current is maintained during cold events.

7. Conclusions

[50] This high resolution multiproxy investigation of cores across the subpolar North Atlantic first clearly identifies the fraction of the sediment originating from the basaltic rocks essentially located around Iceland. Proxies identified on a regional scale for this common source are magnetic concentration, smectite percentage and titanium content. The coeval variations of all these parameters in each core indicate that they were all transported in a similar way from the northern source southward. The transport vector invoked here for this basaltic fraction is the bottom current and the observed fluctuations with time illustrate changes in the strength of this bottom current along the flow path of North Atlantic Deep Water. This interpretation is strongly corroborated by the grain size data illustrating stronger bottom current activity during warm periods (interstadial) than during cold ones (Heinrich event and stadials).

[51] The Norwegian Sea also recorded the changes in the strength of the deep current implying that the overflow was active during interstadials. This suggests that an open ocean convection was dominant in the Norwegian Sea during interstadials. This is consistent with the dynamic described by models, oscillating between a "warm mode" during interstadials and a "glacial mode" during stadials and Heinrich events. The deep water formed during this open ocean convection was then overflowed into North Atlantic *via* the main gateways and propagated downstream.

Acknowledgments

[52] This study has been conducted in the framework of the international IMAGES program. We express our thanks to the crew of the R/V *Marion Dufresne* as well as the French Polar Institute (IPEV). Laurent Labeyrie, Claude Hillaire-Marcel, and Jean-Louis Turon were the Chief Scientists of the 1995 and 1999 cruises. S. Hemming and an anonymous referee are gratefully acknowledged for their help in improving the manuscript. Sharyn Crayford (NIOZ) checked the English language. Aurélie van Toer and Olivier Dufour helped with the laboratory analyses. M.B. acknowledges a grant from the French Ministry of Research. This work was supported by the Commissariat à l'Energie Atomique (CEA), the Centre National de la Recherche Scientifique (CNRS), and the Programme National d'Etudes du Climat (VAGALAM Project). This is LSCE contribution 1748.

References

Alley, R. B., and P. U. Clark (1999), The deglaciation of the northern hemisphere: A global perspective, *Annu. Rev. Earth Planet. Sci.*, *27*, 149–182.

Behairy, A. K., R. Chester, A. J. Griffiths, L. R. Johnson, and J. H. Stoner (1975), The clay mineralogy of particulate material from some surface seawaters of the eastern Atlantic Ocean, *Mar. Geol.*, *18*, M45–M46.

Berry, R., and W. Johns (1966), Mineralogy of the clay-sized fractions of some North Atlantic-Arctic ocean bottom sediments, *Geol. Soc. Am. Bull.*, *77*, 183–195.

Biscaye, P. E. (1965), Mineralogy and sedimentation of the recent deep-sea clay in the Atlantic Ocean and adjacent seas and oceans, *Geol. Soc. Am. Bull.*, *76*, 803–831.

Bond, G., W. Broecker, S. Johnsen, J. McManus, L. Labeyrie, J. Jouzel, and G. Bonani (1993), Correlation between climate records from North Atlantic sediments and Greenland ice, *Nature*, *365*, 143–147.

Chamley, H. (1989), *Clay Sedimentology*, 623 pp., Springer, New York.

Colin, C., A. Bertaux, A. Desprairies, L. Turpin, and C. Kissel (1999), Erosional history of the Himalayan and Burman ranges during the last two glacial-interglacial cycles, *Earth Planet. Sci. Lett.*, *171*, 647–660.

Curry, W. B., T. M. Marchitto, J. F. McManus, D. W. Oppo, and K. L. Laarkamp (1999), Millennial changes in the ventilation of the thermocline, Intermediate, and Deep Waters of the Glacial North Atlantic, in *Mechanisms of Global Climate Changes at Millennial Time Scales*, *Geophys. Monogr. Ser.*, vol. 112, edited by P. U. Clark, R. S. Webb, and L. D. Keigwin, pp. 59–76, AGU, Washington, D. C.

Day, R., M. Fuller, and V. A. Schmidt (1977), Hysteresis properties of titano-magnetite: Grain size and compositional dependence, *Phys. Earth Planet. Inter.*, *13*, 260–267.

Dokken, T., and E. Jansen (1999), Rapid changes in the mechanism of ocean convection during the last glacial period, *Nature*, *401*, 458–461.

Elliot, M., L. Labeyrie, G. Bond, E. Cortijo, J. L. Turon, N. Tisnerat, and J. C. Duplessy (1998), Millennial-scale iceberg discharges in the Irminger Basin during the last glacial period: Relationship with the Heinrich events and environmental settings, *Paleoceanography*, *13*, 433–446.

Elliot, M., L. Labeyrie, T. Dokken, and S. Manthé (2001), Coherent patterns of ice-rafted debris deposits in the Nordic regions during the last glacial (10–60 ka), *Earth Planet. Sci. Lett.*, *194*, 151–163.

Elliot, M., L. Labeyrie, and J. C. Duplessy (2002), Changes in North-Atlantic deep-water formation associated with the Dansgaard-Oeschger temperature oscillations (10–60 ka), *Quat. Sci. Rev.*, *21*, 1153–1165.

Evans, M. E., and F. Heller (2003), *Environmental Magnetism: Principles and Applications of Enviromagnetics*, *Int. Geophys. Ser.*, vol. 86, 299 pp., Elsevier, New York.

Fagel, N., and C. Hillaire-Marcel (1997), Changes in the Western Boundary Undercurrent outflow since the Last Glacial Maximum, from smectite/illite ratios in deep Labrador Sea sediments, *Paleoceanography*, *12*, 79–96.

Fagel, N., C. Robert, and C. Hillaire-Marcel (1996), Clay mineral signature of the NW Atlantic Boundary Undercurrent, *Mar. Geol.*, *130*, 19–28.

Fagel, N., C. Robert, M. Preda, and J. Thorez (2001), Smectite composition as a tracer of deep circulation: The case of the Northern North Atlantic, *Mar. Geol.*, *172*, 309–330.

Ganopolski, A., and S. Rahmstorf (2001), Rapid changes of glacial climate simulated in a coupled climate model, *Nature*, *409*, 153–158.

Gehrke, B., K. S. Lackschewitz, and H.-J. Wallrabe-Adams (1996), Late Quaternary sedimentation on the Mid-Atlantic Reykjanes Ridge: Clay mineral assemblages and depositional environment, *Geol. Rundsch.*, *85*, 525–535.

Griffin, J. J., H. Windom, and E. Goldberg (1968), The distribution of clay minerals in the world ocean, *Deep Sea Res. Oceanogr. Abstr.*, *15*, 433–459.

Grousset, F. E., C. Latouche, and M. Parra (1982), Late quaternary sedimentation between the Gibbs Fracture Zone and the Greenland Basin: Mineralogical and geochemical data, *Mar. Geol.*, *47*, 303–330.

Jansen, J. H. F., S. J. Van Der Gaast, B. Koster, and A. Vaars (1998), CORTEX, a shipboard XRF scanner for element analyses in split sediment cores, *Mar. Geol.*, *151*, 143–153.

Keigwin, L. D., and E. A. Boyle (1999), Surface and deep ocean variability in the Northern Sargasso Sea during marine isotope stage 3, *Paleoceanography*, *14*, 164–170.

Kent, D. V. K., S. R. Hemming, and B. D. Turrin (2002), Laschamp excursion at Mono Lake?, *Earth Planet. Sci. Lett.*, *197*, 151–164.

Kissel, C. (2005), Magnetic signature of rapid climatic variations in glacial North Atlantic: A review, *C. R. Geosci.*, *337*, 908–918.

Kissel, C., C. Laj, L. Labeyrie, T. Dokken, A. Voelker, and D. Blamart (1999a), Rapid climatic variations during marine isotopic stage 3: Magnetic analysis of sediments from Nordic Seas and North Atlantic, *Earth Planet. Sci. Lett.*, *171*, 489–502.

Kissel, C., C. Laj, L. Labeyrie, T. Dokken, A. Voelker, and D. Blamart (1999b), Magnetic signature of rapid climatic variations in North Atlantic sediments, in *Reconstructing Ocean History: A Window Into the Future*, edited by F. Abrantes and A. Mix, pp. 419–437, Springer, New York.

Labeyrie, L., H. Leclaire, C. Waelbroeck, E. Cortijo, J. C. Duplessy, L. Vidal, M. Elliot, B. Le Coat, and G. Auffret (1999), Temporal variability of the surface and deep waters of the northwest Atlantic Ocean at orbital and millennial scales, in *Mechanisms of Global Climate Changes at Millennial Time Scales*, *Geophys. Monogr. Ser.*, vol. 112, edited by P. U. Clark, R. S. Webb, and L. D. Keigwin, pp. 77–98, AGU, Washington, D. C.

Lackschewitz, K. S., H.-J. Wallrabe-Adams, and D. Garbe-Schönberg (1994), Geochemistry of surface sediments from the mid-oceanic Kolbeinsey Ridge, north of Iceland, *Mar. Geol.*, *121*, 105–119.

Laj, C., C. Kissel, A. Mazaud, J. E. T. Channel, and J. Beer (2000), North Atlantic paleointensity stack since 75 ka (NAPIS 75) and the duration of the Laschamp event, *Philos. Trans. R. Soc. London, Ser. A*, *358*, 1009–1025.

Latouche, C., and M. Parra (1976), Minéralogie et géochimie des sédiments quaternaires de l'Océan Atlantique nord-oriental (Mer de Norvège-golfe de Gascogne)—Essais d'interprétations sédimentologiques, *Mar. Geol.*, *22*, 33–69.

Latouche, C., and M. Parra (1979), La sédimentation au Quaternaire récent dans le "Northwest Atlantic Mid-Ocean Canyon"—Apport des données minéralogiques et géochimiques, *Mar. Geol.*, *29*, 137–164.

Lavrov, V. M., V. K. Nikolayeva, and M. S. Barash (1971), Titanium in the quaternary deposits of the Atlantic Ocean, *Oceanology*, *13*, 57–62.

Manthe, S. (1998), Variabilité de la circulation thermohaline glaciaire et interglaciaire tracée par les foraminifères planctoniques et de la microfaune benthique, Ph.D. thesis, 289 pp., Univ. de Bordeaux I, Bordeaux, France.

McCave, I. N., B. Manighetti, and S. G. Robinson (1995), Sortable silt and fine size/composition slicing: Parameters for paleocurrent speed and paleoceanography, *Paleoceanography*, *10*, 593–610.

Moreno, E., N. Thouveny, D. Delanghe, I. N. McCave, and N. J. Shackleton (2002), Climatic and oceanographic changes in the Northeast Atlantic reflected by magnetic properties of sediments deposited on the Portuguese Margin during the last 340 ka, *Earth Planet. Sci. Lett.*, *202*, 465–480.

Moros, M., R. Endler, K. S. Lackschewitz, H. J. Wallrabe-Adams, J. Mienert, and W. Lemke (1997), Physical properties of Reykjanes Ridge sediments and their linkage to high resolution Greenland Ice Sheet Project 2 ice core data, *Paleoceanography*, *12*, 687–695.

Moros, M., A. Kuijpers, I. Snowball, S. Lassen, D. Bäckström, F. Gingele, and J. McManus (2002), Were the glacial iceberg surges in the North Atlantic triggered by climatic warming?, *Mar. Geol.*, *192*, 393–417.

Parra, M. (1980), Apport des données minéralogiques et géochimiques à la connaissance de la sédimentation profonde et de l'hydrologie de l'Océan Nord-Atlantique pendant le Quaternaire terminal (dernier glaciaire et post-glaciaire), Ph.D. thesis, 242 pp., Univ. de Bordeaux I, Bordeaux, France.

Parra, M., C. Puechmaille, J. C. Dumon, P. Delmont, and A. Ferragne (1986), Geochemistry of tertiary alterite clay phases on the Iceland-Faeroe Ridge (northeast Atlantic), leg 38, site 336, *Chem. Geol.*, *54*, 165–176.

Petersen, L., and K. Rasmussen (1980), Mineralogical composition of the clay-size fraction of two fluvio-glacial sediments from east Greenland, *Clay Miner.*, *15*, 135–145.

Pouthier, J., and E. Gonthier (1978), Sur la susceptibilité magnétique des sédiments, indicateurs de la dispersion du matériel volcanoclastique à partir de l'Islande et des Faeroes, *Bull. Inst. Géol. Aquitaine*, *23*, 214–226.

Prins, M. A., L. M. Bouwer, C. J. Beets, S. R. Troelstra, G. J. Weltje, R. W. Kruk, A. Kuijpers, and P. Z. Vroon (2002), Ocean circulation and iceberg discharge in the glacial North Atlantic: Inference from unmixing of sediment distributions, *Geology*, *30*, 555–558.

Rasmussen, T. L., E. Thomsen, L. Labeyrie, and T. C. E. Van Weering (1996a), Circulation changes in the Faeroe-Shetland Channel correlating with cold events during the last glacial period 58–10 ka BP, *Geology*, *24*, 937–940.

Rasmussen, T. L., E. Thomsen, T. C. E. Van Weering, and L. Labeyrie (1996b), Rapid changes in the surface and deep water conditions at the Faeroe Margin during the last 58,000 ka, *Paleoceanography*, *11*, 757–771.

Rasmussen, T. L., E. Thomsen, and T. C. E. Van Weering (1998), Cyclic sedimentation on the Faeroe Drift 53–10 ka BP related to climatic variations, in *Geological Process on Continental Margins: Sedimentation, Mass-Wasting and Stability*, edited by M. S. Stoker, D. Evans, and A. Cramp, *Geol. Soc. Spec. Publ.*, *129*, 255–267.

Rateev, M. A., Z. N. Gorbunova, A. P. Lisitizin, and G. L. Nasov (1969), The distribution of the clay minerals in the oceans, *Sedimentology*, *13*, 21–43.

Revel, M., M. Cremer, F. E. Grousset, and L. Labeyrie (1996), Grain-size and Sr-Nd isotopes as tracer of paleo-bottom current strength, Northeast Atlantic Ocean, *Mar. Geol.*, *131*, 233–249.

Richter, T. O., S. J. Van der Gaast, B. Koster, A. Vaars, R. Gieles, H. C. de Stigter, H. de Haas, and T. C. E. van

Weering (2005), The Avaatech XRF Core Scanner: Technical description and applications to NE Atlantic sediments, in *New Ways of Looking at Sediment Cores and Core Data*, edited by G. Rothwell, *Geol. Soc. Spec. Publ.*, in press.

Robinson, S. G., M. A. Maslin, and N. McCave (1995), Magnetic susceptibility variations in Upper Pleistocene deep-sea sediments of the NE Atlantic: Implication for ice rafting and paleocirculation at the last glacial maximum, *Paleoceanography*, *18*(2), 1026, doi:10.1029/2001PA000732.

Sarnthein, M., et al. (2000), Fundamental modes and abrupt changes in North Atlantic circulation and climate over the last 60 ky—Concepts, reconstruction and numerical modeling, in *The Northern North Atlantic: A Changing Environment*, edited by P. Schäfer et al., pp. 365–410, Springer, New York.

Snowball, I., and M. Moros (2003), Saw-tooth pattern of North Atlantic current speed during Dansgaard-Oeschger cycles revealed by the magnetic grain size of the Reykjanes Ridge sediments at 59°N, *Paleoceanography*, *18*, 1–12.

Stoner, J., J. E. T. Channel, and C. Hillaire-Marcel (1996), The magnetic signature of rapidly deposited detrital layers from the deep Labrador Sea: Relationship to North Atlantic Heinrich layers, *Paleoceanography*, *11*, 309–325.

Tauxe, L., J. L. LaBreque, R. Dodson, M. Fuller, and J. Dematteo (1983), "U"-channels: A new technique for paleomagnetic analysis of hydraulic piston cores, *Eos Trans. AGU*, *64*, 219.

Vidal, L., L. Labeyrie, E. Cortijo, M. Arnold, J. C. Duplessy, E. Michel, S. Becqué, and T. C. E. van Weering (1997), Evidence for changes in the North Atlantic Deep Water linked to meltwater surges during the Heinrich events, *Earth Planet. Sci. Lett.*, *146*, 13–27.

Vidal, L., L. Labeyrie, and T. C. E. van Weering (1998), Benthic $\delta^{18}O$ records in the North Atlantic over the last glacial period (60–10! kyr): Evidence for brine formation, *Paleoceanography*, *13*(3), 245–251.

Wagner, G., J. Beer, C. Laj, C. Kissel, J. Masarik, R. Muscheler, and H.-A. Synal (2000), Chlorine evidence for the Mono Lake event in the Summit GRIP ice core, *Earth Planet. Sci. Lett.*, *181*, 1–6.

Watkins, S. J., and B. A. Maher (2003), Magnetic characterisation of present-day deep-sea sediments and sources in the North Atlantic, *Earth Planet. Sci. Lett.*, *214*, 379–394.

Weeks, R., C. Laj, L. Endignoux, M. Fuller, A. Roberts, R. Manganne, E. Blanchard, and W. Goree (1993), Improvements in long core measurement techniques: Applications in paleomagnetism and paleoceanography, *Geophys. J. Int.*, *114*, 651–662.